Reactive Landing of Gas-Phase Ions as a Tool for the Fabrication of Metal Oxide Surfaces for In Situ Phosphopeptide Enrichment

Grady R. Blacken, Michael Volný,* Matthew Diener, Karl E. Jackson, Pratistha Ranjitkar, Dustin J. Maly, and František Tureček
Department of Chemistry, University of Washington, Seattle, Washington, USA

Zirconium, titanium, and hafnium oxide-coated stainless steel surfaces are fabricated by reactive landing of gas-phase ions produced by electrospray ionization of group IVB metal alkoxides. The surfaces are used for in situ enrichment of phosphopeptides before analysis by matrix-assisted laser desorption ionization (MALDI) mass spectrometry. To evaluate this method we characterized ZrO_2 (zirconia) surfaces by (1) comparison with the other group IVB metal oxides of TiO_2 (titania) and HfO_2 (hafnia), (2) morphological characterization by SEM image analysis, and (3) dependence of phosphopeptide enrichment on the metal oxide layer thickness. Furthermore, we evaluated the necessity of the reactive landing process for the construction of useful metal oxide surfaces by preparing surfaces by electrospray deposition of Zr, Ti, and Hf alkoxides directly onto polished metal surfaces at atmospheric pressure. Although all three metal oxide surfaces evaluated were capable of phosphopeptide enrichment from complex peptide mixtures, zirconia performed better than hafnia or titania as a result of morphological characteristics illustrated by the SEM analysis. Metal oxide coatings that were fabricated by atmospheric pressure deposition were still capable of in situ phosphopeptide enrichment, although with inferior efficiency and surface durability. We show that zirconia surfaces prepared by reactive landing of gas-phase ions can be a useful tool for high throughput screening of novel phosphorylation sites and quantitation of phosphorylation kinetics. (J Am Soc Mass Spectrom 2009, 20, 915–926) © 2009 American Society for Mass Spectrometry

Many cellular processes including metabolism, transcription, and differentiation are largely controlled by reversible protein phosphorylation [1]. Kinases, phosphorylating enzymes, and phosphatases, dephosphorylating enzymes, are able to modulate phosphorylation of serine, threonine, and tyrosine residues, causing dynamic changes in protein structure and function. It has been estimated that 30–50% of all proteins in eukaryotic organisms are phosphorylated at any time [2]. Given the extensive role of phosphorylation in the human body, it is perhaps surprising that the human genome codes for only about 520 kinases (1–2% of the genome) out of 24,500 coding genes [3]. Of these 520 kinases, 244 have been mapped to disease or cancer-causing conditions—thus understanding their function can be of great use for designing therapies and cures for many human ailments.

The typical phosphoproteomics workflow [4] often involves growing target cells under two conditions: a control and a perturbed condition [5]. The proteins formed either can be labeled in the cell culture, using approaches such as stable isotopic labeling of amino acids in cell culture (SILAC) [6], or the purified proteins can be modified after extraction using isotope-coded affinity tag (ICAT) based derivatization methods [7, 8]. After labeling, the differentially expressed proteins can be subjected to either global proteomics analysis or a targeted analytical approach. In the former technique the extracted proteins are digested and analyzed by liquid chromatography mass spectrometry (LC-MS) without any further purification. This global bottom-up approach requires either a targeted detection strategy using tandem mass spectrometry [9–15] or the use of high-resolution, high-capacity mass analyzers.

Although global and top-down proteomics strategies are becoming increasingly more possible, targeted strategies are still necessary to achieve meaningful biological conclusions [4, 5]. Targeted phosphoproteomics involves several stages of enrichment and selective purification to isolate desired biomolecules. The first stage involves phosphoprotein enrichment or immunoprecipitation (IP) to isolate the phosphoproteome. This is usually followed by two-dimensional electrophoretic separation on a sodium dodecyl sulfate polyacrylamide

Address reprint requests to Dr. František Tureček, University of Washington, Department of Chemistry, Bagley Hall, Box 351700, Seattle, WA 98195-1700. E-mail: turecek@chem.washington.edu

* Present address: Laboratory of Molecular Structure Characterization, Academy of Sciences of the Czech Republic, Videnska 1083, Prague 4, 14220 Czech Republic.

1044-0305/09/$32.00
doi:10.1016/j.jasms.2009.01.006

Published online January 22, 2009
Received October 31, 2008
Revised January 11, 2009
Accepted January 13, 2009

gel (2D-SDS-PAGE) to isolate individual phosphoproteins or, more likely, groups of proteins that might be contained in a single gel band. These bands can then be sliced out and reconstituted for tryptic digestion to smaller peptides, of 8–14 amino residues, that are more amenable to MS analysis. Once the target protein or proteins are isolated, the peptides might then be subjected to further enrichment to purify the tryptic phosphopeptides from the complex digest. This purification step is often necessary before MS analysis because of the high complexity of biological samples, the large dynamic range of phosphorylation, and the typically low ionization efficiency of phosphorylated peptides compared with the nonphosphorylated forms [5]. Phosphopeptide enrichment has undergone significant growth over the past two decades as a result of both the successes and the limitations of immobilized metal-ion affinity chromatography (IMAC) [16–18]. The IMAC strategy typically involves a metal chelating resin, such as agarose derivatized with nitrilotriacetic acid (NTA), loaded with a phosphate-selective metal such as Ga^{3+} or Fe^{3+}. When peptide or protein samples are applied to this column, the phosphorylated residues are selectively retained, whereas the nonphosphorylated forms can be washed away. This technique is rapid, inexpensive, and effective and thus remains a very popular tool for phosphopeptide enrichment in proteomics analyses.

Several limitations exist for IMAC techniques resulting in sample complexity by nonspecific binding to the column. The main issues include (1) the capture of peptide acidic residues such as aspartic acid, glutamic acid, or the C-terminus and (2) capture of hydrophobic residues by the gel bead. The first problem was initially addressed by Ficarro et al. [17], who demonstrated that carboxylate methyl esterification could block the nonspecific capture of acidic residues. The derivatization also allows for the incorporation of an isotopic label useful for quantitation. The technique is widely used, although its continued growth is hampered by the yield of the derivatization reaction. Specifically, incomplete methyl esterification leads to increased sample complexity and signal dilution of individual peptide ions [19]. Thus, the field of phosphoproteomics is still seeking to simplify and improve on current techniques for phosphopeptide enrichment.

More recently, metal oxide affinity chromatography (MOAC) has begun to rival IMAC in utility with phosphoproteomic applications. Originally described in 2004, titanium dioxide columns were used to selectively enrich phosphopeptides from complex samples, including the *Drosophila melanogaster* proteome [20, 21]. Zirconia, another group IVB metal oxide, has also proved to be useful as a phosphopeptide enrichment material [22]. The benefit of MOAC columns is the ability to withstand extreme solution conditions, including the use of organic acids to aid in phosphopeptide binding specificity and low pH binding and washing conditions [23]. MOAC columns can be loaded and washed in up to 5% trifluoroacetic acid (TFA), allowing for efficient protonation of peptide carboxylates. IMAC columns, on the other hand, cannot be exposed to low p*K*a binding conditions because the NTA moiety will be protonated and the metal leached from the column. The effect is that phosphopeptides must be bound to IMAC columns at pH values near or above the p*K*a of peptide carboxylates, leaving many Asp and Glu residues deprotonated and capable of nonspecific binding.

Two recent comparative studies illustrate the need to evaluate each enrichment technique for a particular application because IMAC and MOAC are both capable of complementary and distinct phosphopeptide enrichment. In one study of the *D. melanogaster* phosphoproteome, the digested protein sample was subjected to three separate phosphopeptide enrichment strategies: IMAC, MOAC, and covalent capture via phosphoramidate chemistry [24]. This study found that the three techniques were able to enrich complementary portions of the fruit fly phosphoproteome. Alternately, a separate study has found that TiO_2 chromatography was superior to both ZrO_2 and IMAC [25]. In that study, the enhanced stability of MOAC in several loading and washing buffers was demonstrated. The advantage of TiO_2 over ZrO_2 was not elucidated and was presumably attributed only to differences in the manufacturing process. Regardless, it is clear that the choice of enrichment strategy may be an empirical decision unique to each application.

We have recently reported on the utility of stainless steel surfaces coated with a durable layer of zirconia for the efficient enrichment of phosphopeptides directly on matrix-assisted laser desorption ionization (MALDI) sample plates [26]. By detecting the phosphopeptides directly from the MALDI surfaces our method eliminates complications associated with phosphopeptide elution and allows for automated, high-throughput MALDI analyses. Furthermore, the rapid enrichment on these surfaces allows for an additional stage of chromatographic separation to be performed in a matter of minutes with minimal volumes of solvent. Thus the technique presented here will fit well with the online, multistage separations, before MALDI-MS analysis, that have become standard in proteomics [27–29]. The surfaces are generated by exposing plasma-oxidized stainless steel surfaces to collisions with gas-phase cations generated by electrospray ionization (ESI) of zirconium(IV)-*n*-propoxide. This robust and highly reproducible surface preparation process lends itself to a variety of applications [30–33].

Here we evaluate the phosphopeptide enrichment capabilities of several metal oxide coatings. First, we compare zirconia with the other group IVB metal oxides titania and hafnia. We use scanning electron microscope (SEM) image analysis to show how enrichment may be related to surface morphology. Second, we evaluate the effect of metal oxide surface thickness on phosphopeptide enrichment. Finally, we compare our soft and reactive-landing preparation

technique with a simplified, bench-top method for metal oxide surface preparation.

Experimental

Materials

Titanium(IV)-*n*-butoxide, zirconium(IV)-*n*-propoxide, and hafnium(IV)-*n*-propoxide were obtained from Sigma–Aldrich (Milwaukee, WI, USA) as 70% solutions in 1-propanol. Solvents were purchased from Fisher Scientific (Pittsburgh, PA, USA). The peptides used to characterize phosphopeptide enrichment on the zirconium oxide functional surfaces include the synthetic peptides NQLLpTPLR, MpSGIFR, MSGIFR, and pY-WQAFR, purchased from Genscript Corporation (Piscataway, NJ, USA), and peptides from the tryptic digestion of α-casein. Sequence-grade trypsin and α-casein were purchased from Sigma–Aldrich. The tryptic digestion of α-casein was performed at a 1:20 enzyme-to-substrate weight ratio in 50 mM NH_4HCO_3 and incubated overnight at 37 °C. Organic acids used as MALDI matrixes (α-cyano-4-hydroxycinnamic acid [CHCA] and 2,5-dihydroxybenzoic acid [DHB]) were purchased from Sigma–Aldrich.

MALDI-TOF/TOF Mass Spectrometry

MALDI mass spectra were acquired on an Applied Biosystems 4700 Proteomics Analyzer system (Applied Biosystems, Carlsbad, CA, USA), operated in positive-ion mode. Optimum precursor ion signals in MALDI/time-of-flight (TOF)-MS analyses, operated with the reflector on, were acquired with matrix solutions consisting of either 1 mg/mL CHCA in 50% acetonitrile with 1% phosphoric acid (PA) or 1 mg/mL DHB in 50% acetonitrile with 1% PA. The relatively dilute concentrations of organic matrix are necessary to create a thin crystal layer so that phosphopeptides bound to the metal oxide surface may be accessible to laser desorption.

Alteration of Standard MALDI Plates

A standard stainless steel MALDI plate was modified by milling off several layers of material from the area of about 20 × 20 mm and 2 mm depth to accommodate the Zr-oxide–coated substrate plates. The substrate plate was mounted inside the depression with adhesive tape and thus leveled with the rest of the MALDI plate surface. In principle, reactive landing could be done on the MALDI plate directly, without having to mount externally prepared surfaces. Reasons for our current approach include the higher price of commercial MALDI plates and the fact that smaller chips of cut stainless steel are easier to handle inside the soft-landing instrument, which has relatively narrow chambers [30].

Scanning Electron Microscopy (SEM)

Images were acquired on the FEI Sirion SEM system in the nanotechnology user facility at the University of Washington. Before analysis, gold was sputter-coated onto the surface for 30 s at a rate of 7 nm/min to build a 3.5-nm-thick conducting layer to account for the low conductivity of the metal oxide. Optimal resolution occurred using a 7-keV incident electron beam. An energy-dispersive X-ray (EDX) photon detector equipped on the SEM system allowed for localization of metal oxide on the stainless steel surfaces.

Surfaces

Metal targets used as substrates for deposition of group IVB metal dioxides were made of roughly 15 × 15-mm 316L stainless steel plates. The plates were mechanically polished with a diamond paste; rinsed successively with hexane, methanol, and water; sonicated in 1:1 chloroform/methanol for 15 min; rinsed with methanol; and exposed to oxygen plasma immediately after cleaning.

In Situ Plasma Treatment

The custom-made plasma reactor is similar to that described by Ratner [34] and was operated at 13.56 MHz. It is an integral part of the soft and reactive landing instrument as described previously [30]. The surface treatment was carried out at 60-W radio-frequency power for 10 min in 250 mTorr of flowing oxygen gas.

Preparation of Surfaces by Reactive Landing

For reactive landing experiments, 70% metal alkoxide in 1-propanol was diluted in the same solvent to the final concentration of 10 μM. The solution was electrosprayed in positive mode and the ions were landed on a freshly plasma-treated stainless steel surface. The landing experiment lasted between 1.5 and 6 h and the landing substrate was biased at −50 V, corresponding to a landing energy of 50 eV for singly charged ions. The gas-phase ions consisted of a mixture of alkoxylated Zr, Ti, or Hf clusters, similar to those reported for negative-ion electrospray of Zr(IV) alkoxides. The cations were not mass-separated before reactive landing. The sample surface was then removed from the instrument and further examined. The landed material forms a compact spot that is visible to the naked eye (Figure 1, bottom, inset). The spot was successively rinsed with water, methanol, propanol, and hexane and then soaked in a water/propanol mixture for 4 h. All samples that were prepared and used in this study did not visibly change upon multiple washings. The Zr-oxide coating remained intact even after it was rubbed with wet soft material such as filtration paper or cotton wool.

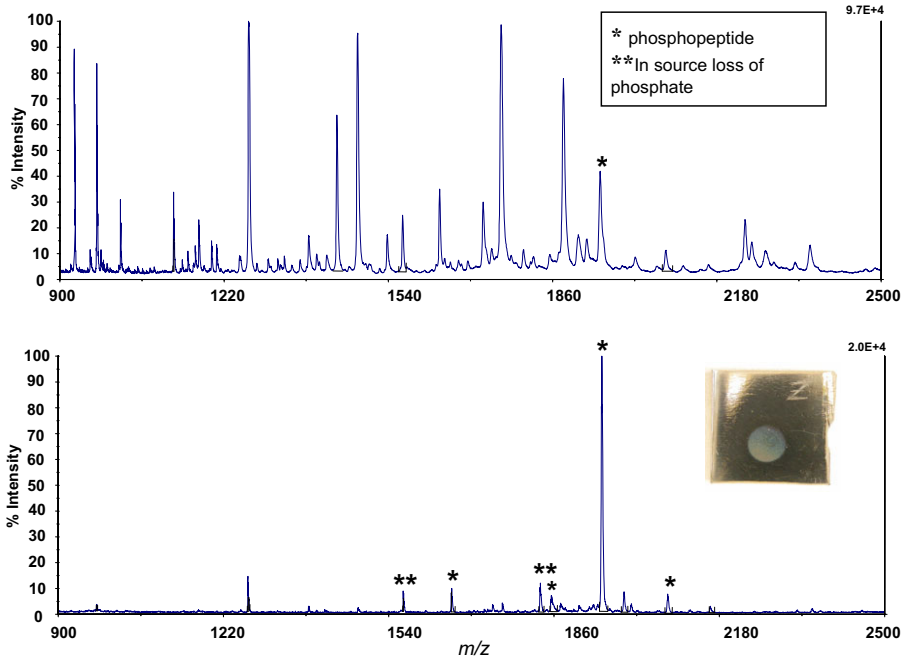

Figure 1. MALDI-TOF mass spectrum of a tryptic digestion of 2:1 (mol/mol) BSA:alpha casein. Complete analysis of complex mixture (top) is compared with in situ enrichment (bottom) for phosphopeptides on zirconia surfaces prepared by reactive landing of zirconium *n*-propoxide. The metal oxide forms a visible spot on the stainless steel surface (bottom, inset). The phosphopeptide ions are denoted by single asterisk. Double asterisks denote dissociation products by elimination of phosphoric acid.

Preparation of Surfaces by "Bench-top" Atmospheric Pressure ESI

The bench-top apparatus is depicted in Scheme **1**.

Briefly, a stainless steel shim was polished and cleaned by plasma treatment as described earlier. After plasma treatment the shim was removed from the plasma chamber and attached to the bench-top ESI apparatus. The surfaces were heated to between 170 and 200 °C before application of metal oxide through the ESI needle. Such temperatures were required for adhesion of the metal oxide to the stainless steel surface. The needle was held at 3 kV while the surface was held at ground potential. Metal oxide deposition time was also varied between 5 and 15 min, with little effect on surface appearance or phosphopeptide enrichment capabilities. Deposition times beyond 15 min resulted in accumulation of unbound and unusable metal oxide.

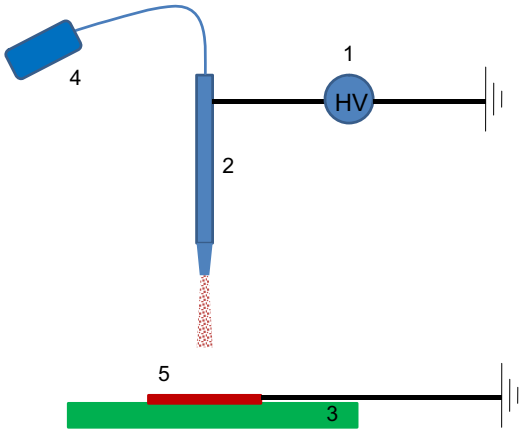

Scheme 1. Diagram of setup for a bench-top apparatus open to the atmosphere that could be used for construction of zirconia surfaces on plasma treated stainless steel. (1) High-voltage power supply at 3 kV with respect to ground, (2) spray needle, (3) heated block with temperature control, (4) syringe pump with metal alkoxide solution, (5) target plate.

Phosphopeptide Enrichment

In preparation for phosphopeptide enrichment the surfaces were washed by agitating in 10 mL aliquots of methanol (3 times), 100 mM NH_4OH (2 times, 10 min each), water (3 times), and then equilibrated in a wash/bind solution consisting of an aqueous mixture of 20% acetonitrile and 0.1% TFA. Peptide mixtures, diluted to the desired concentration in the wash/bind solution, were then applied to the assay surface and incubated at room temperature for 20 min. Approximately 10 min after application, each peptide spot was mixed with a micro-pipettor by drawing in and expelling the droplet back onto the original assay surface. After 20 min of incubation the spots were washed with the wash/bind solution either by applying and removing several 30 μL portions of wash/bind solution to the assayed surface or by immersing and agitating the surface in 25 mL of the wash/bind solution for 2 min. After the final wash

the surfaces were allowed to dry and matrix was spotted directly onto the assayed area.

Src Phosphorylation Assays

A construct protein containing the catalytic domain was expressed in *E. coli*, purified and treated with a phosphatase to ensure quantitative dephosphorylation [35, 36]. Before digestion, the c-Src protein was denatured and reduced with 6 M urea and 10 mM dithiothreitol at 60 °C for 1 h. After cooling and diluting 6-fold in 50 mM ammonium bicarbonate the enzyme was alkylated with 10 mM iodoacetamide for 15 min in the dark. Trypsin was added at a 1:20 trypsin to c-Src ratio and the digestion was allowed to proceed overnight at 37 °C. Each digest was quenched with TFA and desalted over a C18 ziptip (Waters Corp., Milford, MA, USA) using an aqueous solution of 20% acetonitrile/0.1% TFA as eluent. Aliquots (1 pmol) of each of the desalted digests were spotted onto different locations on the same zirconia-coated MALDI plate for phosphopeptide enrichment. The plate was fabricated by manipulating the surface mount inside the soft-landing instrument to raster across the Zr ion beam, creating the fully coated surface of approximately 1 × 1 cm. On this surface all six digests, resulting from each time point, could be simultaneously enriched for the analyte and internal standard phosphopeptides and washed in a single step by dipping into aqueous 20% acetonitrile/0.1% TFA.

Results and Discussion

Phosphopeptide Enrichment on Ti and Hf Metal Oxides

To determine optimal conditions for in situ phosphopeptide enrichment on MALDI surfaces we first sought to compare the utility of zirconia coatings with other group IVB metal oxides, specifically titania and hafnia. The selective binding of phosphorylated residues to these surfaces relies on hard Lewis acid/base chemistry. Each metal center in the group IVB metal dioxides, with the metal in the 4+ charge state, exhibits the characteristics of a hard Lewis acid. Thus, interactions are largely ionic in character between the Zr^{4+}, Ti^{4+}, or Hf^{4+} ions and the negative, doubly charged phosphate. The common solid forms of these dioxides exhibit similar molar densities with titania and zirconia being nearly identical—7.33×10^5 and 7.89×10^5 mol/m^3, respectively—whereas hafnia is slightly more dense at 9.3×10^5 mol/m^3 [37]. Thus, variation in phosphopeptide enrichment capabilities may be more a function of bulk and morphological properties of the solid coatings as opposed to physical differences of the metal centers. Such bulk properties can be visualized by SEM image analysis to offer insight into the nature of the relative utility of various metal oxide coatings for phosphopeptide enrichment.

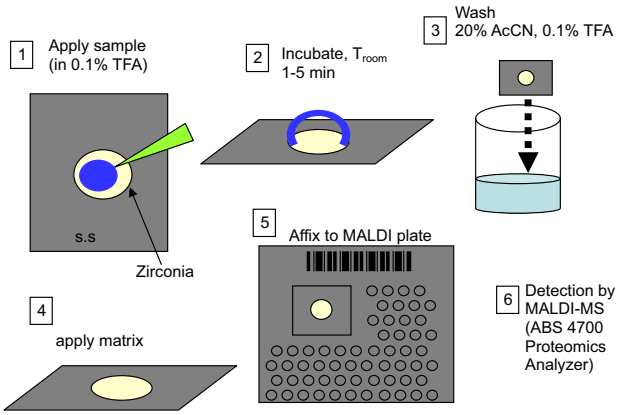

Scheme 2. Illustration of procedure for in situ phosphopeptide enrichment on a MALDI plate. Stainless steel shims are coated with zirconia by soft/reactive landing of electrospray ionized zirconia propoxide. Peptide solutions can be applied and unbound portions washed away before bound phosphopeptides are directly detected by laser desorption ionization assisted by CHCA or DHB matrices. Data acquired on ABS 4700 Proteomics Analyzer.

To compare phosphopeptide enrichment capabilities of various metal oxide surfaces we used a standard tryptic digest of a 2:1 (mol/mol) mixture of bovine serum albumin (BSA) and alpha casein. Each enrichment was performed by applying 1 pmol of an alpha casein tryptic digestion (2 pmol BSA) to a metal oxide surface with the diameter of a standard MALDI plate (~1.5 mm). The digest solution was buffered to 0.1% TFA to allow for optimal selectivity for phosphopeptide capture on the enrichment surface. Scheme **2** illustrates the procedure for enrichment of such mixtures on a stainless steel surface coated with zirconia. The alpha casein, singly phosphorylated peptide, with one tryptic miscleavage, appears as the most intense signal in the enriched spectrum at *m/z* 1951. The full tryptic peptide also appears as an intense signal at *m/z* 1660. The doubly phosphorylated peptide is detected with a metastable loss of one phosphate at *m/z* 1827. Only the most abundant phosphopeptide, at *m/z* 1951, could be discerned among abundant nonphosphorylated peptides in the nonenriched spectrum in Figure 1.

Initially, three different metal oxide surfaces—titania, zirconia, and hafnia—each prepared using the soft-landing technique were compared for phosphopeptide enrichment capabilities. Each surface used for this comparison was prepared by soft landing of a 10 μM solution of the respective metal alkoxide, dissolved in 1-propanol, onto plasma-treated stainless steel for 3 h at a flow rate of 100 μL/h. The data in Figure 2 indicate that zirconia provides the greatest phosphopeptide capture and detection efficiency when compared with titania and hafnia prepared under similar soft-landing conditions. SEM image analysis reveals some interesting morphological differences between these three surfaces, which may hint at their relative utility for phosphopeptide enrichment. Areas of uncoated stainless

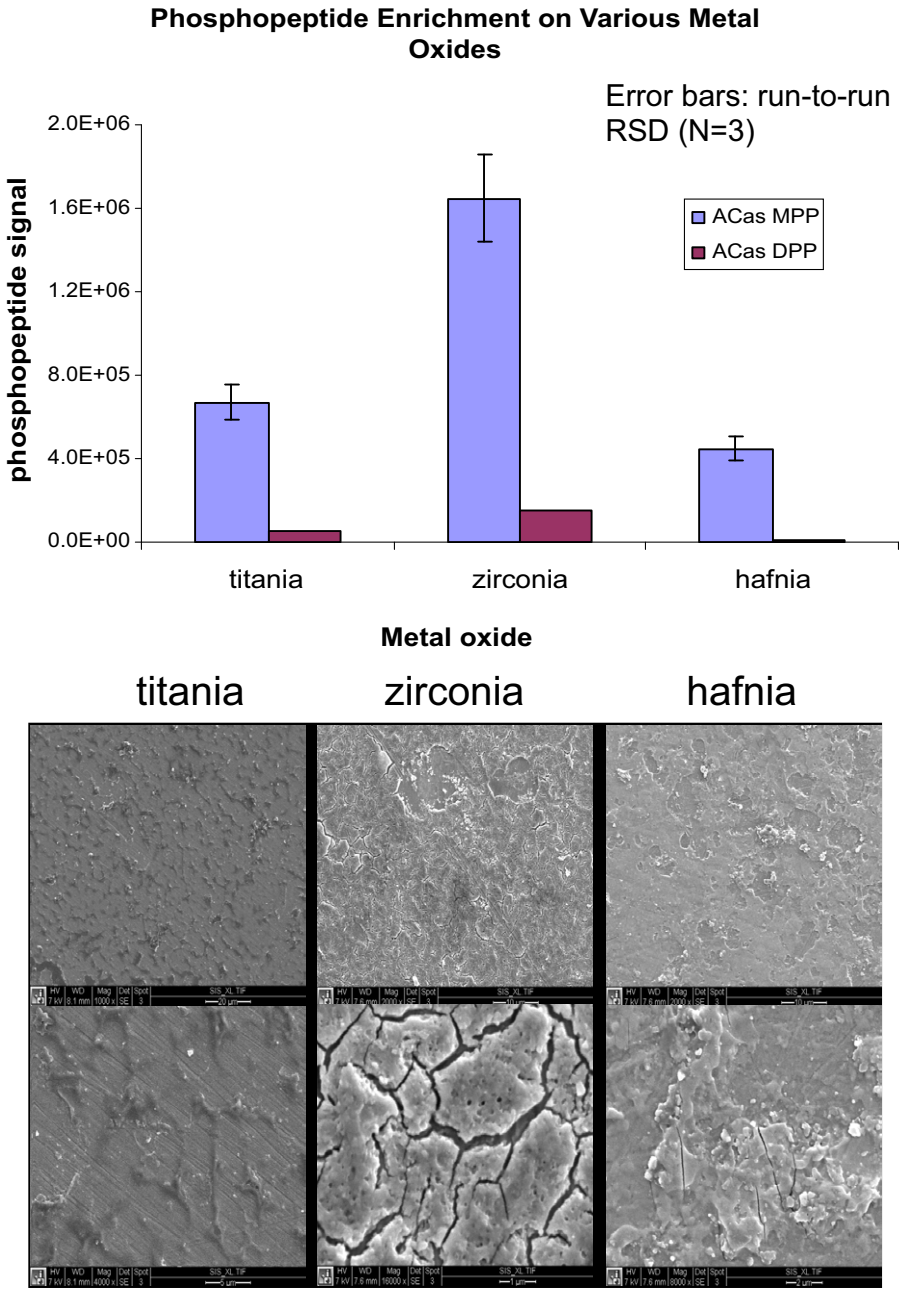

Figure 2. The group IVB metal oxides are compared for relative ability to enrich phosphopeptides. Analysis of the same sample described in Figure 1 on titania, zirconia, and hafnia reveals that zirconia is able to selectively enrich the alpha casein diphosphorylated (DPP, residues 58–73) and monophosphorylated peptides (MPP, residues 119–134) more efficiently than hafnia or titania (top). SEM analysis (bottom) reveals that zirconia provides an optimal balance of surface coverage and morphological features optimal for phosphopeptide-metal oxide binding.

steel can be visualized as portions of the surface containing machined lines, most notable on the titania surface. Not only can the metal oxide areas be visualized as the nonmachined portions, but confirmation of these areas as metal oxide was carried out by EDX analysis with the energy-dispersed spectrometer equipped on the FEI Sirion SEM system (Figure S1, Supplementary Material, which can be found in the electronic version of this article).

From visual inspection of the SEM images, we can make several inferences about the relative ability of these metals to enrich for phosphopeptides. The titania surface is marked by features that appear as ridges of metal oxide on the stainless steel surface. The excessive distance between these ridges, about 5–15 μm, decreases surface coverage while at the same time perhaps exposing larger areas of metal oxide than a more uniform coating. In contrast, the hafnia forms a more

continuous surface layer, providing more surface coverage than titania but perhaps still a comparable metal oxide surface area because of the presence of fewer morphological features. By comparison, zirconia appears to offer an optimal balance of surface coverage and metal oxide surface area. The increased presence of cracks and pores relative to the hafnia surface and the improved surface coverage relative to the titania surface make zirconia more desirable for phosphopeptide enrichment, as a result of increased capacity and optimal chromatography. Indeed the nature of the differences in metal oxide structure between these three surfaces is likely specific to the soft-landing method of metal oxide surface preparation. This is probably true of all metal oxide preparation techniques in that it has been observed that the relative enrichment performance of metal oxides is dependent on the manufacturer and manufacturing process.

Phosphopeptide Enrichment Depends on the Zirconia Surface Thickness

Next, we studied the phosphopeptide enrichment efficiency as a function of zirconia coating thickness. To vary the thickness we varied the amount of metal oxide that was soft-landed on the surface while maintaining the same spot area, which is determined by ion focusing in the fringing field of the octopole ion guide. The signal-to-noise ratio for three synthetic phosphopeptides—NQLLpTPLR, pYWQAFR, and MpSGIFR—was used to compare the phosphopeptide enrichment on these surfaces as a function of the soft-landing time used for metal oxide surface preparation. Three different surfaces were fabricated for this comparison so that separate pieces of polished and plasma-treated stainless steel were subjected to soft landing of electrosprayed zirconium propoxide for 1.5, 3, and 6 h. Figure 3 illustrates that phosphopeptide enrichment increases directly with soft-landing time and thus metal oxide thickness. This is to be expected since, as shown by the SEM analysis, the zirconia coating is characterized by cracks and pores that can only deepen and increase as more zirconia is deposited. So the phosphopeptides are apparently able to "soak" into and bind the metal oxide surface while still being accessible for laser desorption and ionization with MALDI. The direct dependence of phosphopeptide enrichment on deposition time means that more efficient and cheaper methods for surface construction will better facilitate the construction of large numbers of high-capacity surfaces for a high-throughput phosphorylation site screening by in situ enrichment on MALDI plates.

Reactive Landing Surface Preparation versus Simplified Bench-top Technique

To this end, we evaluated the utility of our reactive landing technique by comparison with surfaces prepared

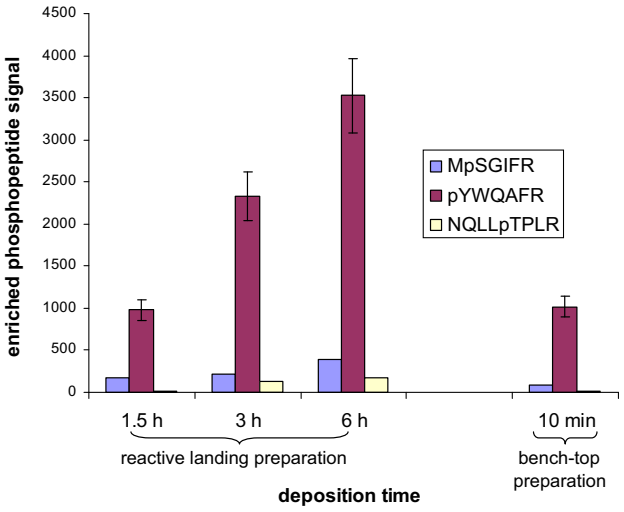

Figure 3. Comparison of phosphopeptide enrichment on zirconia surfaces prepared under various conditions. Enrichment efficiency increases proportionally with reactive landing time, whereas enrichment on surfaces prepared by the bench-top design is not dependent on zirconia deposition time. Plasma cleaned stainless steel surface was heated to 170 °C before deposition with the bench-top apparatus. Error bars indicate run-to-run relative standard deviations (RCDs) in triplicate measurements ($N = 3$).

by ESI with a bench-top setup that is fully open to the atmosphere. The latter technique was evaluated to potentially offer a simple method of surface construction that might bypass the high vacuum and ion optics of the soft and reactive landing instrument. The stainless steel substrates were polished and plasma treated as described earlier. We have observed that simply drying zirconium(IV)-*n*-propoxide on the plasma-treated stainless steel surface does not result in a usable coating because the zirconia does not adhere to the stainless steel [26]. Furthermore, ESI onto plasma-cleaned but otherwise untreated stainless steel surfaces, at atmospheric pressure and room temperature, produced no permanent zirconia coating. Thus, we conclude that to form an adherent Zr-oxide coating on the target surface the Zr-carrying ions must strike the surface at the hyperthermal kinetic energies (e.g., 50 eV), such as those produced by our reactive landing method.

We have attempted to overcome the complications with the simple atmospheric pressure ESI technique by preheating the plasma-cleaned metal surfaces. Heating allows us to compensate for collisional cooling with atmospheric gases, simulating the high-energy landing environment of the soft and reactive landing instrument. The surface preparation procedure is illustrated in Scheme **1**. A 10 μM solution of zirconium propoxide in 1-propanol was electrosprayed at 100 μL/h directly onto the grounded and heated metal surfaces, through a capillary held at 3 kV. After 10 min of deposition, significant accumulation of white zirconia was observed. When the surface was preheated below 100 °C

the zirconia layer durability was significantly diminished and was not retained on the surface. Heating the surfaces to between 170 and 200 °C resulted in functional surfaces that could be used for phosphopeptide enrichment.

Within this range of preheated substrate temperatures used for zirconia surface preparation, the phosphopeptide capture efficiency of the respective zirconia coatings was observed to decrease with increasing temperature. SEM image analysis shows a more amorphous physical structure for the coatings prepared at higher temperature (Figure S2). The relative phosphopeptide enrichment efficiencies of these surfaces prepared under various conditions are also illustrated in Figure 3. This chart shows that phosphopeptide enrichment on the surfaces prepared with the bench-top technique compares with enrichment on the thinnest and least efficient zirconia surfaces prepared by reactive landing. Furthermore, enrichment capabilities for the surfaces prepared by the simplified technique were not found to vary with deposition time beyond 5 min of electrospray coating at atmospheric pressure. Thus, the enrichment efficiency could not be improved by increasing deposition time with the bench-top setup as it was possible under reactive landing conditions. This is probably attributable to the different structure of the material formed by the atmospheric pressure method. Phosphopeptide enrichment on the surfaces prepared by the bench-top ESI method may be useful for applications requiring a phosphorylation site screening of samples of relatively low complexity or those known to contain high-abundance phosphopeptides. Conversely, the reactive landing conditions for zirconia surface preparation will provide the more efficient, higher-capacity phosphopeptide enrichment surface.

Quantification of Kinase Kinetics Using In Situ Phosphopeptide Enrichment

We demonstrate the utility of phosphopeptide enrichment on zirconia-coated MALDI plates by quantitative measurements of the effects of various stimuli on phosphorylation kinetics. One example of this is the screening of small-molecule kinase inhibitors that may affect enzyme activity and thus allow for control of various cellular processes. Numerous methods currently exist for such studies that typically include scintillation-based detection of phosphorylation events derived from incorporation of radioactive, ^{32}P-labeled adenosine 5′-triphosphate (ATP). Although typically very sensitive, these methods give no information about phosphorylation site location and carry the added costs and hazards associated with the use of radioactive materials. Thus, more informative and less hazardous quantitation by MS is advantageous to these scintillation-based detection techniques.

We applied our technique to monitor the kinetics of the autophosphorylation of the tyrosine kinase c-Src (Figure S3). Src undergoes autophosphorylation at the Tyr-416 residue within its activation loop (KVADFGLARLIEDNEYTARQGAK) [38], which provides a phosphorylated LIEDNEpYTAR tryptic peptide after digestion. Phosphorylation was carried out by incubating 1 μM protein in 100 μM ATP for various amounts of time. After 0, 5, 10, 20, 30, and 60 min, aliquots of the assay were removed and added to 1 equivalent of internal standard peptide LIEDNEpYTVR in 1% TFA, to halt the kinase activity. The internal standard differs from the target peptide in one hydrophobic residue only (V instead of A) and is expected to have a similar response in MALDI. This was tested by MALDI-MS analysis of a 1:1 mixture of both peptides where the response factor for the LIEDNEpYTAR analyte peptide was about 40% of that of the LIEDNEpYTVR internal standard. The relative responses to the analyte and internal standard were used to determine the adjusted relative response (see Figure 5).

Figure 4 shows that quantitation by MALDI-MS analysis is significantly enhanced with the use of phosphopeptide enrichment. Quantitation of phosphorylation kinetics is possible using the nonenriched sample, assuming the interfering peptide is at a constant concentration in all assay time points. This appears to be true since the assay follows a similar trend in both the enriched and the nonenriched samples. The relative error, determined by triplicate analyses of the 20-min time point, indicates that no error is introduced by phosphopeptide enrichment. Rather, the phosphopeptide enrichment surfaces can be used for rapid and facile clean-up of such samples for quantitative analyses. Furthermore, the time-dependent plot in Figure 5 agrees well with a study by Sun et al. [39], who performed the same kinetic analysis using a traditional, targeted radioactive labeling and scintillation counting method. The relative standard deviation in our kinetic measurements is comparable to the standard error of MALDI measurements reported by Applied Biosystems for the 4700 proteomics analyzer [40]. Thus, analysis-to-analysis variability was not significantly affected by phosphopeptide enrichment on zirconia-coated MALDI plates. It should be noted that our internal standard was related to the analyte by a residue substitution (V for A) and was not an isotopically labeled analogue of the analyte peptide.

Although scintillation-based assays may be more sensitive, the obvious advantage of performing phosphorylation kinetics analyses using the MALDI-MS platform is the phosphorylation site information that may be useful for troubleshooting such assays. For example, at physiological concentrations of ATP (2–5 mM) it has been observed that Src can be deactivated in the absence of other enzymes. Src has a known regulatory phosphorylation site whose phosphorylation by the tyrosine kinase Csk causes down-regulation of this

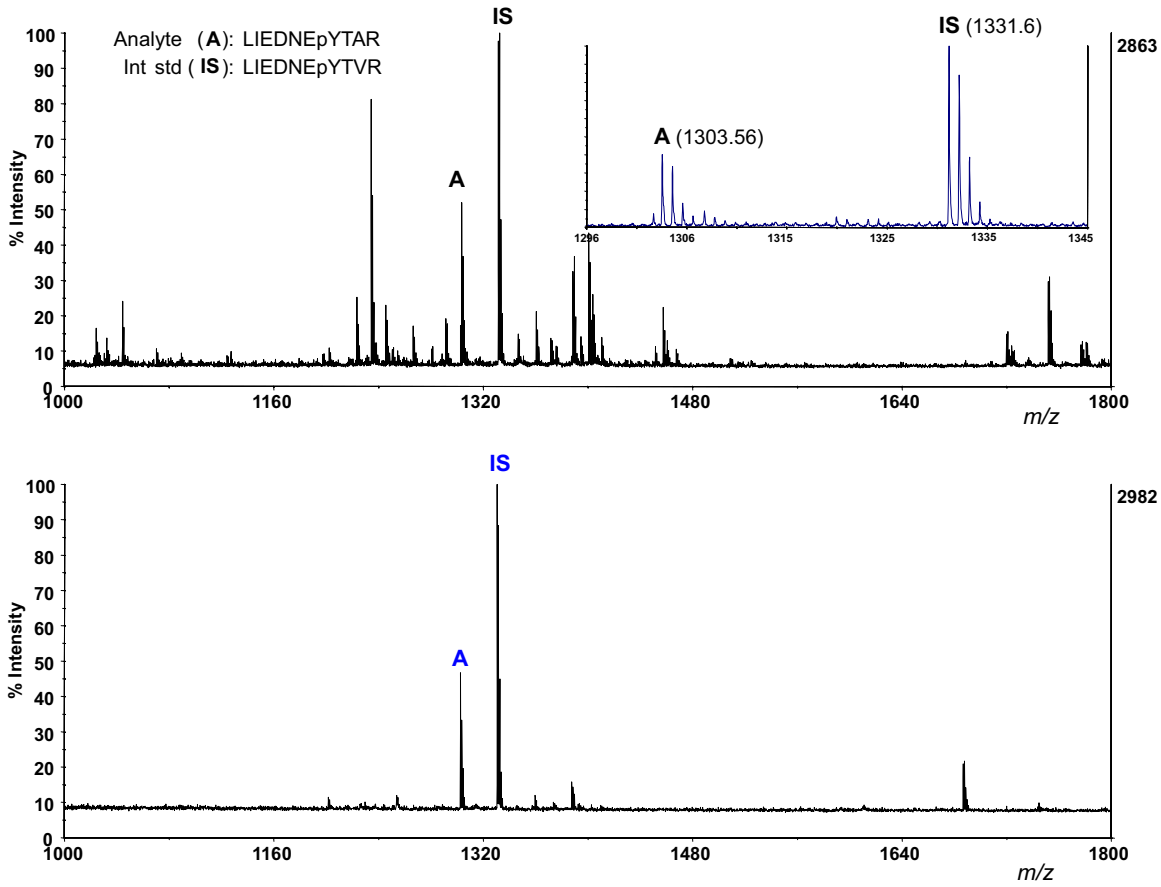

Figure 4. Top: Tryptic digest of the protein tyrosine kinase chicken Src phosphorylated for 60 min in 100 μM ATP. Bottom: The same sample was enriched (1 pmol per 1.5-mm diameter MALDI spot) on zirconia-coated stainless steel. The analyte tryptic peptide, LIEDNEpYTAR, is labeled with A. The internal standard peptide, LIEDNEpYTVR, is labeled with IS. Small peaks in the bottom spectrum corresponding to addition of 57 u to the A and IS peak are from overreaction with iodoacetamide during alkylation before tryptic digestion.

enzyme. In the absence of Csk this site is not phosphorylated in vitro under kinetically controlled conditions (<100 μM ATP). However, under higher, more physiologically relevant ATP concentrations this regulatory site can be autophosphorylated and is detected by MALDI-MS analysis. In fact the autophosphorylation of the Src regulatory site (Tyr-527) was predicted by a previous study [35] and is compatible with the detection of a tryptic peptide at *m/z* 4064 in the MALDI-MS spectrum, which likely corresponds to a long C-terminus tryptic segment containing a phosphorylated Tyr-527 residue (Figure 6). We note that this large tryptic peptide did not survive flight through the post-source tube and thus could not be resolved by the TOF reflector and isolated for MS/MS characterization. Nevertheless, the *m/z* value was indicative of the phosphorylation site. The inability to observe phosphorylation of this regulatory site would lead to confusion as to how activity is lost in the absence of regulatory enzymes. A scintillation-based detection method, such as that used in traditional kinase assays, cannot provide adequate information to illustrate this issue.

Conclusions

Zr-oxide surfaces provide a useful tool for the in situ enrichment and detection of phosphopeptides by MALDI-TOF mass spectrometry. In particular, Zr-oxide–coated spots that were prepared by reactive landing of Zr(IV)-*n*-propoxide ions on stainless steel substrates proved to be efficient in enriching singly phosphorylated peptides in mid-femtomole amounts for both synthetic peptide mixtures and protein tryptic digests. Enrichment factors about 20- to 90-fold were achieved when compared with the abundant nonphosphopeptides. The Zr-oxide–coated surfaces showed good reproducibility, even after having been reused up to 20 times without significant loss in enrichment efficiency. An advantage of Zr-oxide coatings is that they can be produced on stainless steel supports in a variety of sizes by focusing or defocusing the ion beam used for reactive landing.

Further characterization of the reactively landed Zr-oxides and other group IVB transition-metal oxides was evaluated for their ability to enrich phos-

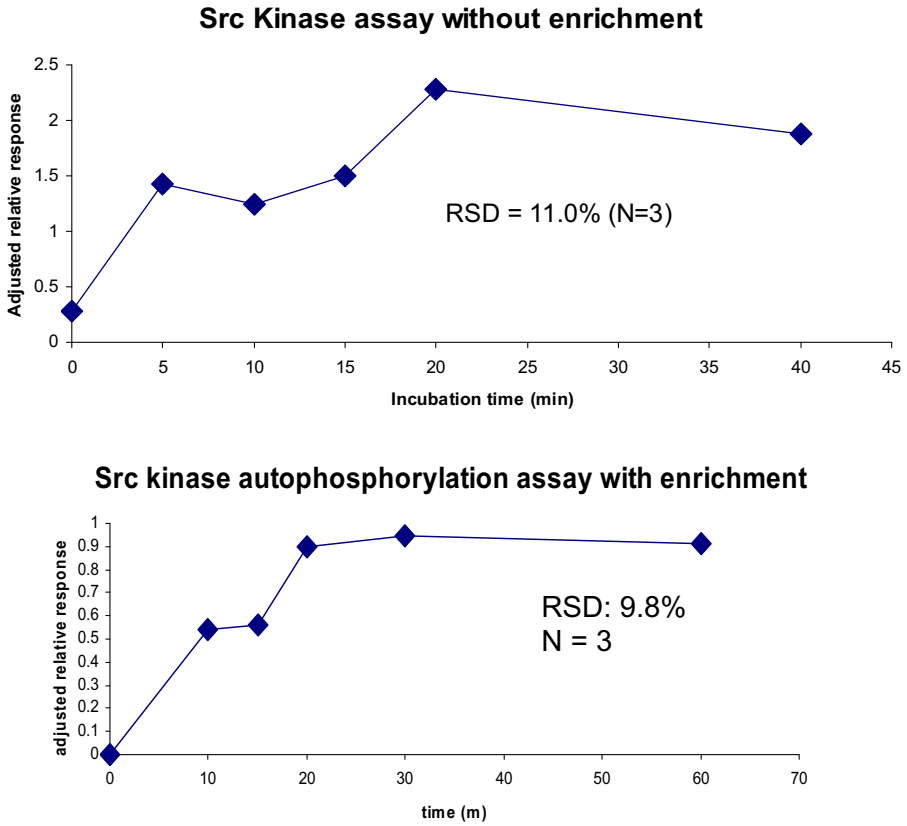

Figure 5. Quantitation of Src kinase autophosphorylation kinetics without (top) and with (bottom) phosphopeptide enrichment on zirconia. Without enrichment, an interfering peptide inflates the analyte signal, although to a somewhat constant amount, allowing for relative error comparison between the two quantitative assays. Enrichment on zirconia-coated MALDI plates does not add error relative to nonenriched assays.

phopeptides. It was shown that, using our reactive landing surface preparation technique, zirconia is superior to titania, which is in turn superior to hafnia in terms of phosphopeptide enrichment efficiency. This is likely explained by morphological differences as observed by SEM image analysis. Furthermore, it is observed that enrichment efficiency is directly proportional to reactive landing time and thus metal

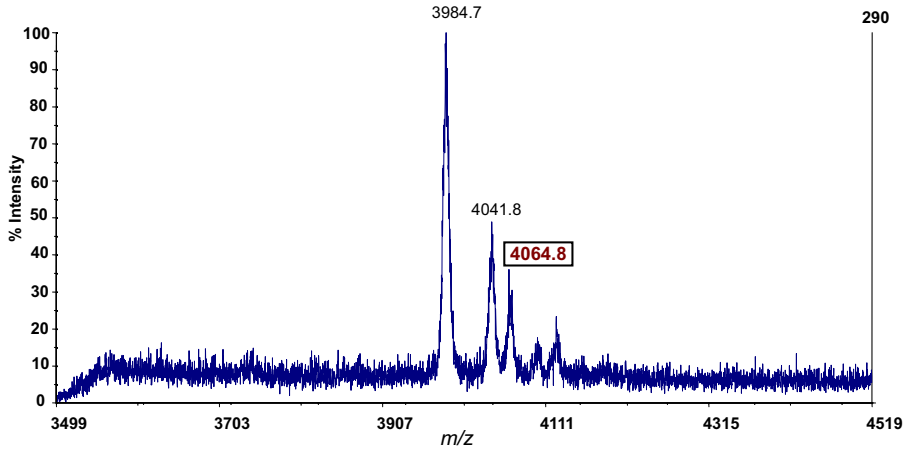

Figure 6. Autophosphorylation of the Src regulatory site Tyr-527 is detected by MALDI-MS analysis of a tryptic digest of the enzyme after it has been treated with ATP and $MgCl_2$ for 30 min in an aqueous buffered solution. The tryptic peptide corresponding to the regulatory phosphorylation site (*m/z* 4066.8) is identified by in situ enrichment on a zirconia-coated MALDI plate and TOF-MS in linear mode.

oxide thickness. This trend likely illustrates the ability of analyte molecules to diffuse into the metal oxide layer, thus accessing a larger surface area than if diffusion were not possible. Since the enrichment efficiency of these zirconia surfaces depends on the reactive landing deposition time, we then also attempted to make a rapid and simplified, bench-top surface construction technique. Phosphopeptides were in fact enriched on these surfaces, although a >3-fold increase in efficiency was achieved using the reactively landed zirconia surfaces.

Finally, we applied our in situ phosphopeptide enrichment strategy to quantitative phosphorylation kinetics analysis. The zirconia surfaces are able to provide rapid and selective phosphopeptide information that will allow for high-throughput phosphorylation site screening with MALDI-TOF/TOF detection. Quantitation of phosphorylation kinetics is enhanced by enrichment on zirconia surfaces. As shown by data from Src autophosphorylation assays, the in situ phosphopeptide enrichment technique allows for robust and reproducible quantitative information to be gathered. This potentially allows for high-throughput screening of small molecules to target the activity of kinases whose functions may be associated with disease or cancer.

Acknowledgments

Support by grants for the University of Washington Royalty Research Fund and National Institutes of Health (Grant DK-67869) is gratefully acknowledged.

Appendix A Supplementary Material

Supplementary material associated with this article may be found in the online version at doi:10.1016/j.jasms.2009.01.006.

References

1. Hunter, T. Signaling: 2000 and Beyond. *Cell* **2000,** *100,* 113–127.
2. Kalume, D. E.; Molina, H.; Pandey, A. A. Tackling the Phosphoproteome: Tools and Strategies. *Curr. Opin. Chem. Biol.* **2003,** *7,* 64–69.
3. Manning, G.; Whyte, D. B.; Martinez, R.; Hunter, T.; Sudarsanam, S. The Protein Kinase Complement of the Human Genome. *Science* **2002,** *298,* 1912–1934.
4. Paradela, A.; Albar, J. P. Advances in the Analysis of Protein Phosphorylation. *J. Proteome Res.* **2008,** *7,* 1809–1818.
5. Smith, J. C.; Figeys, D. Proteomics Technology in Systems Biology. *Mol. BioSyst.* **2006,** *2,* 364–370.
6. Ong, S. E.; Blagoev, B.; Kratchmarova, I.; Kristensen, D. B.; Steen, H.; Pandey, A.; Mann, M. Stable Isotope Labeling by Amino Acids in Cell Culture, SILAC, as a Simple and Accurate Approach to Expression Proteomics. *Mol. Cell Proteomics* **2002,** *1,* 376–386.
7. Gygi, S. P.; Rist, B.; Gerber, S. A.; Turečček, F.; Gelb, M. H.; Aebersold, R. Quantitative Analysis of Complex Protein Mixtures Using Isotope Coded Affinity Tags. *Nat. Biotechnol.* **1999,** *17,* 994–999.
8. Goshe, M. B.; Conrads, T. P.; Panisko, E. A.; Angell, N. H.; Veenstra, T. D.; Smith, R. D. Phosphoprotein Isotope-Coded Affinity Tag Approach for Isolating and Quantitating Phosphopeptides in Proteome-Wide Analyses. *Anal. Chem.* **2001,** *73,* 2578–2586.
9. Blacken, G. B.; Gelb, M. H.; Turečček, F. Metal Affinity Capture Tandem Mass Spectrometry for the Selective Detection of Phosphopeptides. *Anal. Chem.* **2006,** *78,* 6065–6073.
10. Blacken, G. R.; Sadilek, M.; Turečček, F. Gallium Metal Affinity Capture Tandem Mass Spectrometry for the Selective Detection of Phosphopeptides in Complex Mixtures. *J. Mass Spectrom.* **2008,** *43,* 1072–1080.
11. Carr, S. A.; Huddleston, M. J.; Annan, R. S. Selective Detection and Sequencing of Phosphopeptides at the Femtomole Level by Mass Spectrometry. *Anal. Biochem.* **1996,** *239,* 180–192.
12. Schroeder, M. J.; Shabanowitz, J.; Schwartz, J. C.; Hunt, D. F.; Coon, J. C. A Neutral Loss Activation Method for Improved Phosphopeptide Sequence Analysis by Quadrupole Ion Trap Mass Spectrometry. *Anal. Chem.* **2004,** *76,* 3590–3598.
13. Chang, E. J.; Archambault, V.; McLachlin, D. T.; Krutchinsky, A. N.; Chait, B. T. Analysis of Protein Phosphorylation by Hypothesis-Driven Multiple-Stage Mass sSectrometry. *Anal. Chem.* **2004,** *76,* 4472–4483.
14. Flora, F. W.; Muddiman, D. C. Gas-Phase Ion Unimolecular Dissociation for Rapid Phosphopeptide Mapping by IRMPD in a Penning Ion Trap: An Energetically Favored Process. *J. Am. Chem. Soc.* **2002,** *124,* 6546–6547.
15. Crowe, M. C.; Brodbelt, J. S. Differentiation of Phosphorylated and Unphosphorylated Peptides by High-Performance Liquid Chromatography-Electrospray Ionization-Infrared Multiphoton Dissociation in a Quadrupole Ion Trap. *Anal. Chem.* **2005,** *77,* 5726–5734.
16. Andersson, L.; Porath, J. Isolation of Phosphoproteins by Immobilized Metal (Fe^{3+}) Affinity Chromatography. *Anal. Biochem.* **1986,** *154,* 250–254.
17. Ficarro, S.; McCleland, M.; Stukenberg, P.; Burke, D.; Ross, M.; Shabanowitz, J.; Hunt, D. F.; White, F. Phosphoproteome Analysis by Mass Spectrometry and Its Application to *Saccharomyces cerevisiae*. *Nat. Biotechnol.* **2002,** *20,* 301–305.
18. Posewitz, M. C.; Tempst, P. Immobilized Gallium(III) Affinity Chromatography of Phosphopeptides. *Anal. Chem.* **1999,** *71,* 2883–2892.
19. Goshe, M. B. Characterizing Phosphoproteins and Phosphoproteomes Using Mass Spectroscopy. *Brief. Funct. Genomic. Proteomic.* **2006,** *4,* 363–376.
20. Pinkse, M. W.; Uitto, P. M.; Hilhorst, M. J.; Ooms, B.; Heck, A. J. Selective Isolation at the Femtomole Level of Phosphopeptides from Proteolytic Digests Using 2D-NanoLC-ESI-MS/MS and Titanium Oxide Precolumns. *Anal. Chem.* **2004,** *76,* 3935–3943.
21. Pinkse, M. W.; Mohammed, S.; Gouw, J. W.; van Breukelen, B.; Vos, H. R.; Heck, A. J. R. Highly Robust, Automated, and Sensitive Online TiO_2-Based Phosphoproteomics Applied to Study Endogenous Phosphorylation in *Drosophila melanogaster*. *J. Proteome Res.* **2008,** *7,* 687–697.
22. Kweon, H. K.; Håkansson, K. Selective Zirconium Dioxide-Based Enrichment of Phosphorylated Peptides for Mass Spectrometric Analysis. *Anal. Chem.* **2006,** *78,* 1743–1749.
23. Larsen, M. R.; Thinghom, T. E.; Jensen, O. N.; Roepstorff, P.; Jorgensen, T. J. D. Highly Selective Enrichment of Phosphorylated Peptides from Peptide Mixtures Using Titanium Dioxide Microcolumns. *Mol. Cell Proteomics* **2005,** *4,* 873–886.
24. Bodenmiller, B.; Mueller, L. N.; Mueller, M.; Domon, B.; Aebersold, R. Reproducible Isolation of Distinct, Overlapping Segments of the Phosphoproteome. *Nat. Methods* **2007,** *4,* 231–237.
25. Jensen, S. S.; Larsen, M. R. Evaluation of the Impact of Some Experimental Procedures on Different Phosphopeptide Enrichment Techniques. *Rapid Commun. Mass Spectrom.* **2007,** *21,* 3635–3645.
26. Blacken, G. R.; Volny, M. E.; Vaisar, T.; Sadilek, M.; Turečček, F. In Situ Enrichment of Phosphopeptides on MALDI Plates Functionalized by Reactive Landing of Zirconium(IV)-*n*-Propoxide Ions. *Anal. Chem.* **2007,** *79,* 5449–5456.
27. Zhai, B.; Villén, J.; Beausoleil, S. A.; Mintseris, J.; Gygi, S. P. Phosphoproteome Analysis of *Drosophila melanogaster* Embryos. *J. Proteome Res.* **2008,** *7,* 1675–1682.
28. Mohammed, S.; Kraiczek, K.; Pinkse, M. W. H.; Lemeer, S.; Benschop, J. J.; Heck, A. J. R. Chip-Based Enrichment and NanoLC-MS/MS Analysis of Phosphopeptides from Whole Lysates. *J. Proteome Res.* **2008,** *7,* 1565–1571.
29. Cantin, G. T.; Yi, W.; Lu, B.; Park, S. K.; Xu, T.; Lee, J.-D.; Yates, J. R., 3rd. Combining Protein-Based IMAC, Peptide-Based IMAC, and MudPIT for Efficient Phosphoproteomic Analysis. *J. Proteome Res.* **2008,** *7,* 1346–1351.
30. Kitching, K. J.; Lee, H.-N.; Elam, W. T.; Turečček, F.; Ratner, B. D.; Johnston, E. E.; MacGregor, H.; Miller, R. Development of an Electrospray Approach to Deposit Complex Molecules on Plasma Modified Surfaces. *Rev. Sci. Instrum.* **2003,** *74,* 4832–4839.
31. Volny, M.; Elam, W. T.; Ratner, B. D.; Turečček, F. Preparative Soft and Reactive Landing of Gas-Phase Ions on Plasma-Treated Metal Surfaces. *Anal. Chem.* **2005,** *77,* 4846–4853.
32. Volny, M.; Elam, W. T.; Branca, A.; Ratner, B. D.; Turečček, F. Preparative Soft and Reactive Landing of Multiply Charged Protein Ions on a Plasma-Treated Metal Surface. *Anal. Chem.* **2005,** *77,* 4890–4896.
33. Volny, M.; Elam, W. T.; Ratner, B. D.; Turečček, F. J. Enhanced In-Vitro Blood Compatibility of 316L Stainless Steel Surfaces by Reactive Landing of Hyaluronan Ions. *J. Biomed. Mater. Res. B* **2007,** *80B,* 505–510.
34. Ratner, B. D. In *Polymeric Materials Encyclopedia*, Salamone, J. C., Ed.; Chemical Rubber Corp.: Boca Raton, FL, 1996; Vol. 11, pp 1006.
35. Sabe, H.; Knudsen, B.; Okada, M.; Nada, S.; Nakagawa, H.; Hanafusa, H. Molecular Cloning and Expression of Chicken c-Src Kinase: Lack of Stable Association with c-Src Protein. *Proc. Natl. Acad. Sci. U. S. A.* **1992,** *89,* 2190–2194.
36. Seeliger, M. A.; Young, M.; Henderson, M. N.; Pellicena, P.; King, D. S.; Falick, A. M.; Kuriyan, J. High yield bacterial expression of active c-Abl and c-Src tyrosine kinases. *Protein Sci.* **2005,** *14,* 3135–3139.

37. Lide, D. R., Ed. *CRC Handbook of Chemistry and Physics*, 87th edition. CRC Press: Boca Raton, FL, 2007.
38. Osusky, M.; Taylor, S. J.; Shalloway, D. Autophosphorylation of Purified c-Src at its Primary Negative Regulation Site. *J. Biol. Chem.* **1995,** *270,* 25729–25734.
39. Sun, G.; Sharma, A. K.; Budde, R. J. A. Autophosphorylation of Src and Yes Blocks Their Inactivation by Csk Phosphorylation. *Oncogene* **1998,** *17,* 1587–1595.
40. For example, see Applied Biosystems application note 114AP20-01 and ABS technical note 114TN49-02 at www.appliedbiosystems.com.